# COHERENT VS. PERSISTENT SCATTERERS: A CASE STUDY.

**L. Marotti[(1)], A. Parizzi[(1)], N. Adam[(1)], K. P. Papathanassiou[(1)]**

[(1)] German Aerospace Center (DLR), Muenchner Strasse 20 82234 Wessling, Germany
Email: luca.marotti@dlr.de

## ABSTRACT

Precise interferometric SAR measurements as well as characterization and information extraction of individual targets can be performed on natural or artificial point-like scatterers in SAR images. This is due, mainly, to the possibility to estimate their phase information very accurately, widely unaffected by speckle. Up to now, by means of two different techniques, two categories of such point-like scatterers have been treated: the Persistent Scatterers (PSs) and the Coherent Scatterers (CSs). On one hand, PSs are characterized by long term temporal stability and are detected using long time series of acquisitions. They enabled the development of geophysical applications as millimetric terrain motion monitoring and accurate DEM refinement. On the other hand, CSs can be detected on a single SAR image basis, by exploiting image spectral correlation properties, without any assumption of temporal stability. They are very promising concerning parameters extraction as LOS rotation angle and dielectric constants estimation. Due to the wide spectrum of informations provided by the combination of the two concepts in this paper we investigate the CSs temporal stability and the relationships existing between CSs and PSs based on the analysis of image time series.

## 1. INTRODUCTION

The accuracy of SAR interferometric measurements is often limited by the uncertainties related with the phase evaluation on a pixel basis. At the same time multiple scattering effects, occurring in the same resolution cell, increase the complexity of the scattering process and make the information extraction from SAR images a challenge. For these reasons, point-like scatterers play an important role in SAR applications as their deterministic response allows an evaluation of their phase information widely unaffected by speckle. Moreover, their deterministic scattering behavior leaves the extraction of informations to be performed in a more direct way. The most prominent class of such point-like scatterers are the so called Permanent Scatterers (PSs) characterized by a long term temporal stability [1]. Accordingly, the identification of PSs is based on the temporal stability of their phase and/or amplitude scattering patterns and relies on the availability of large time series of acquisitions. Their introduction in SAR interferometry enabled the development of millimetric terrain motion monitoring, by measuring Line-of-Sight displacement, as well as the possibility of accurate DEM refinement [1], [4].

More recently, another class of point-like scatterers has been introduced, namely the Coherent Scatterers (CSs) [2]. Their detection is based on their spectral correlation properties and has been addressed in terms of image sub-look (i.e. spectral) correlation. Thus, it can be performed on the basis of single SAR images as long as the system bandwidth is large enough. The deterministic nature of the CSs is linked to their spectral correlation. Indeed, high values of sub-look coherence are related to CSs that represent more closely point-like scatterers while low values of sub-look coherence indicate CSs with a (partial) developed speckle pattern and hence a stochastic scattering behavior. CSs have been explored mainly in terms of their polarimetric properties that have been used to characterize the individual scatterers and to extract information about dielectric properties and physical orientation.

It is important to underline that there is no affirmation of temporal stability involved in the CSs detection, so that CSs and PSs can have a different temporal behavior. While, as mentioned above, PSs temporal stability requires a scattering pattern that does not change in time, the temporal stability of CSs does not necessarily require a stable scattering behavior as long as the deterministic nature of the CSs is not changing.

Towards the combination of the information provided by the two concepts, the question about the temporal stability of CSs has to be answered and the possible complementarities between the two techniques have to be addressed.

Preliminary results about the CSs temporal behavior have been obtained with Quad-Pol data acquired by JAXA' s ALOS-PalSAR [3]. However the lack of sufficient acquisitions did not allow the implementation of PSs detection. In order to investigate this missing

point in understanding the relations between CSs and PSs, in the following we evaluate their relationship based on image time series.

## 2. CSs AND PSs SELECTION

The detection and analysis of the two classes of point-like scatterers is performed processing a stack of 86 C-band ERS1-ERS2 SAR data acquired between 1992 and 2002, with 16 MHz system bandwidth, over the city of Munich in Germany.

In previous studies, the standard CSs detection method has been applied on a single SAR image basis. Accordingly, two sub-look images are created by splitting into two parts the original image range spectrum [2]. Then, the correlation coefficient between the two sub-look images is computed and pixels with high value of sub-look coherence, according to a given threshold, are selected as CSs. Nevertheless, as mentioned in the introduction, this kind of detection approach doesn't take into the availability of a large number of images. Consequently, for the present analysis, the detection procedure has to be performed in a slightly different way.

Fig. 1 shows the temporal evolution of the sub-look coherence value for three different typologies of scatterers described below. As we can observe, the value of sub-look coherence is changing in time depending on the variability of the scattering contributions occurring inside the resolution cell. The red curve is representative of a stable and isolated point-like scatterer that remains dominant in all acquisitions. The blue curve represents a different situation: a stable scattering behavior is obtained after about 20 acquisitions due, probably, to a change in the background scattering within the corresponding resolution cell. Finally, even more variable is the situation described by the green curve. From the above observations we can conclude that a detection procedure performed with a fixed threshold and on a single image basis, that considers as stable scatterers only the points detected in common in all the stack, will discard potential stable CSs even if their value of sub-look coherence drops below the threshold only once on 86 acquisitions.

A more robust detection, that is able to overcome the problem, is described in fig. 2. For each image of the stack the sub-look coherence map is generated and, in the end, the mean sub-look coherence image and the standard deviation image are calculated. Pixels with a high mean value, over a certain threshold, and low standard deviation are considered as CSs. However, since the standard deviation for all the points in this data set is small, within the interval 0-0.2, the effective detection criterion is the mean value.

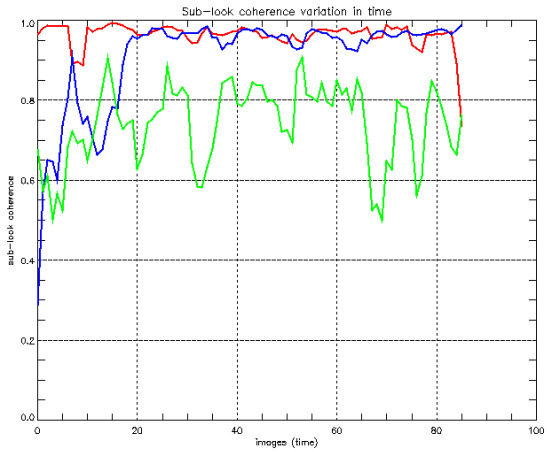


*Figure 1. Time evolution of the sub-look coherence value for a selected CS.*

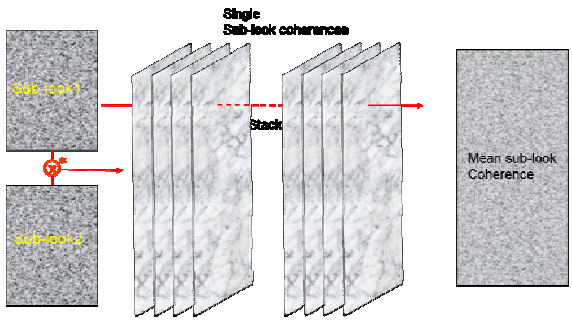


*Figure 2. CSs detection method adapted to a large stack of data.*

As last remark, we can say that for the efficiency of the detection procedure a wide system bandwidth is an advantage for two main reasons. The first is related to the resolution: smaller the resolution cell is the higher the probability to find a dominant scatterer within it becomes. The second reason is related to the fact that in an urban environment the clutter can be partially correlated due to its non ideal Gaussian distribution. In this case a wide system bandwidth is of advantage in order to decrease the probability of false detections caused by possible clutter spectrum correlation. However, the detection of CSs using the relative narrow bandwidth ALOS/PALSAR system (14MHz in the quad-pol mode) has been demonstrated [3] showing the feasibility of the detection procedure by means of ERS data.

Concerning the PSs now, their selection can be performed by means of two criteria: the Dispersion index and the Signal to Clutter ratio. Both approaches estimate the expected phase error based on the SCR. The Dispersion index method [1] is based on the analysis of

the amplitude dispersion of the pixels that it has been shown to be related with the SCR and with the phase error of the corresponding resolution cell. The SCR method [5], used in this work, tries to identify the targets in the image that have a suitable SNR to be considered as PSs. The main idea is to estimate a mean Rayleigh distribution of the clutter surrounding the PS candidate using the realizations of the neighborhood pixels during the whole time span. Finally, as PSs candidate are selected the pixels which have a value of SCR higher than a given threshold. This technique results to be less biased [6] and has the advantage to be able to track the evolution of the SCR in time as depicted in Fig. 3. Clearly we can note that for the selected PS the SCR of the corresponding resolution cell was changing drastically after almost 50 acquisitions.

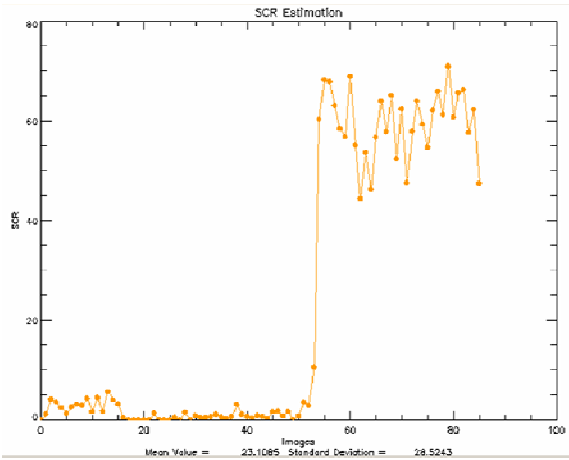


*Figure 3. Time evolution of the SCR value for a selected PS.*

A large amount of PSs (~ 112K) has been selected for the processing choosing a relatively low threshold. At the same time the sub-look coherence threshold has been accordingly adapted to have almost the same amount of CSs detected (~ 111K) for comparison reasons.

The further interferometric processing has been achieved by means of the PSI-GENESIS processor developed at the Remote Sensing Institute (IMF) of DLR [7]. This software module is able to estimate important quantities as deformation velocity displacement, topography and atmospheric contributions. The description of the processing steps is beyond the scope of this paper and in the following will be only briefly summarized. From a subset of the points selected a reference network is constructed and the relative estimations on the single arcs are computed. The network is integrated and the "absolute" estimations per point are extracted. Then, after removing the atmosphere contributions, the estimation is extended to all the points initially selected. Finally by applying a fixed threshold on the quality of the final estimation it is possible to define which points survived the processing and can be considered as PSs.

The same procedure has been performed first on the PSs candidate map and then on the CSs candidate map. The result can be observed in Fig. 4 and Fig. 5 for the PSs and CSs case respectively. It is possible to note that many points, wrongly detected in vegetated regions, have been removed after processing. The final points selected are principally located in the urbanized regions in accordance with the expected deterministic nature of the majority of the man made targets. The parameters analyzed for the CSs-PSs comparison have been calculated on this final set of points.

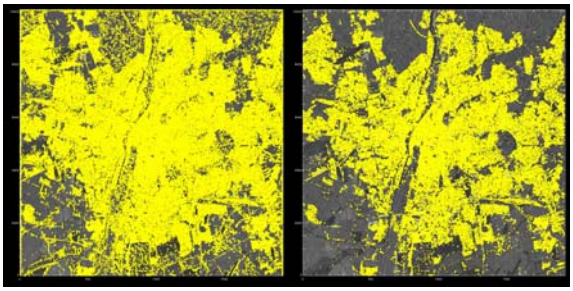

*Figure 4. Left:PSs candidates. Right: final PSs.*

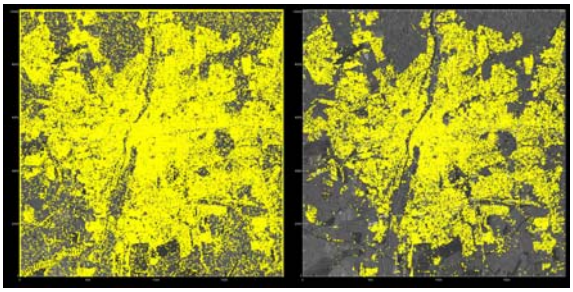

*Figure 5. Left: CSs candidates. Right: final CSs.*

## 3. CSs TIME CHARACTERISTICS

The time period (10 years) covered by the data analyzed in this work allows, for the first time, a founded investigation of the CSs temporal stability. The retrieved number of stable CSs, which survived the interferometric processing, is about 55K. This amount of CSs is comparable with the number of final PSs (about 67K) selected in the dataset. As it will be discussed in the next section, many of the CSs and PSs are located in different positions within the scene giving room to discuss about the possibility to combine the two detection techniques.

The sub-look coherence value used for the CSs detection is a measure of how close to an ideal point scatterer is the response of a target. In Fig. 6 the two dimensional normalized histogram of the correlation between sub-look coherence value and amplitude of the backscattered signal of a resolution cell is shown. The two parameters

have a certain degree of correlation. Indeed, the higher the value of sub-look coherence is the higher will be in general the amplitude. A strong signal component leads the target to be less affected by the phase noise caused by the clutter return. However, a high value of sub-look coherence of 0.8 corresponds to an amplitude range of about 15 dB making amplitude based detection unfeasible.

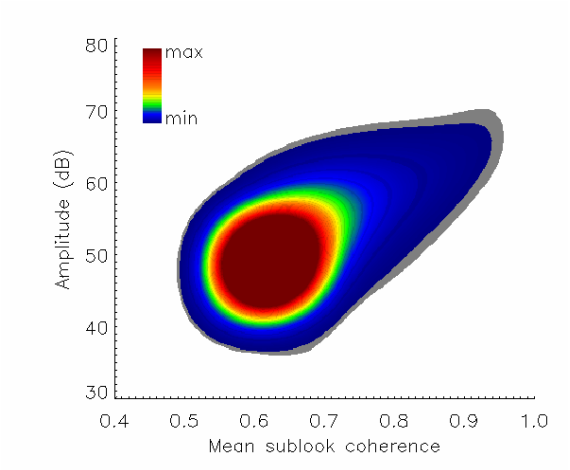


*Figure 6. 2D correlation histogram mean sub-look coherence vs. signal amplitude.*

The correlation between sub-look coherence and the inverse of the dispersion index is showed in Fig. 7. As we can observe, in this case, every value of sub-look coherence corresponds to a wide range of value of dispersion index values probably because a CS doesn't need to have a stable scattering pattern as long as his deterministic nature is not changing.

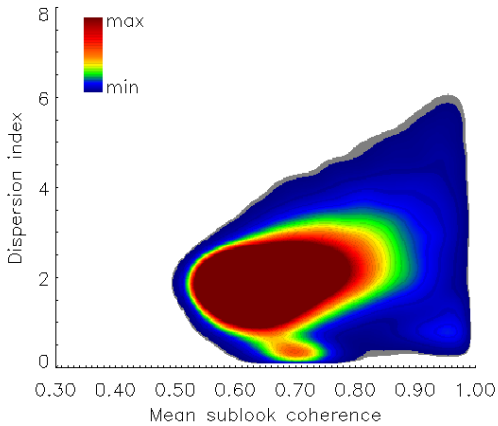


*Figure 7. 2D correlation histogram mean sub-look coherence vs. inverse dispersion index.*

## 4. CSs VS. PSs COMPARISON

Four enlarged images of the scene, corresponding to different regions, are depicted in Fig.8 in order to compare the relative location of the two categories of point-like scatterers.

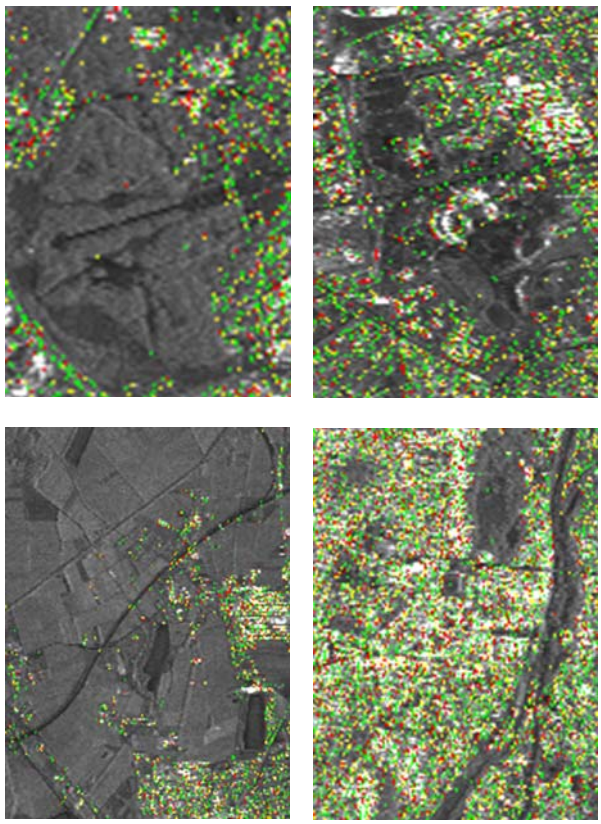

*Figure 8. Detected CSs and PSs in Munich. Upper left: Nynphenburg. Upper right: Olympia Zentrum. Lower left: suburban region. Lower right: city center. Red: CSs. Green: PSs. Yellow: common.*

Red dots correspond to CSs position, green to the PSs position while yellow dots represent the pixels detected using both the techniques. The number of common points detected is surprisingly low (about 25K). This makes clear that it is possible to increase the density of points detected by combining the two approaches. Of course this could be not a strong requirement in urban areas where the density of CSs or PSs is already high but could be helpful in rural regions, for example, where the detection of point-like scatterers is more difficult.

The normalized histogram of the backscattered signal amplitude is drawn in Fig. 9. As expected, both categories of point-like scatterers are, in general, characterized by a higher amplitude compared to the rest of the pixels in the image.

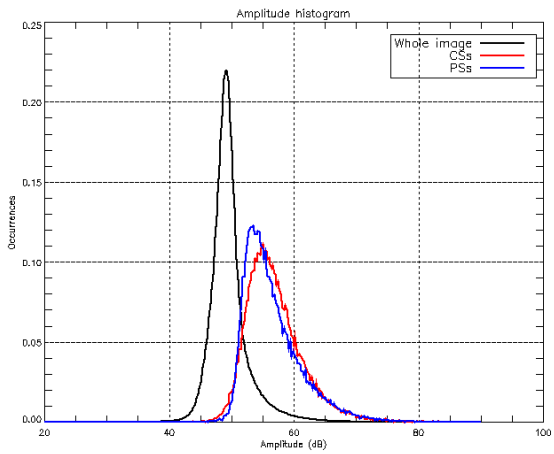


*Figure 9.Amplitude normalized histogram.*

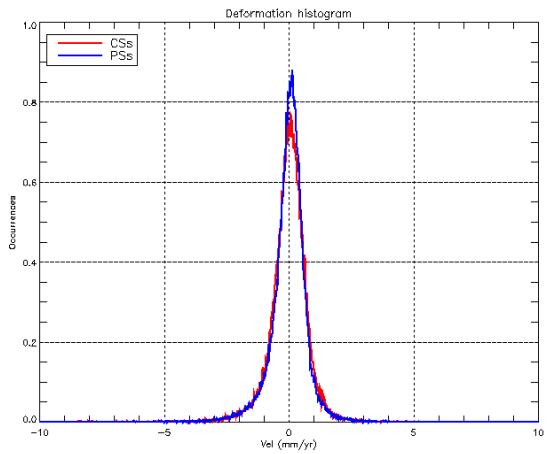


*Figure 11. Normalized histogram of the deformation velocity for CSs (red) and PSs (blue).*

Concerning the LOS deformation velocity, we can see (Fig. 10) that the interferometric processing leads to similar results for both CSs and PSs. The Munich test site results to be very stable with a deformation velocity of less than 1 mm per year. More in detail, in Fig. 11 the normalized histogram of the velocity displacement is depicted calculated on the CSs (red curve) and on the PSs (blue curve). As we can see the result of the interferometric processing, also if performed on points located in different positions, shows a very good agreement.

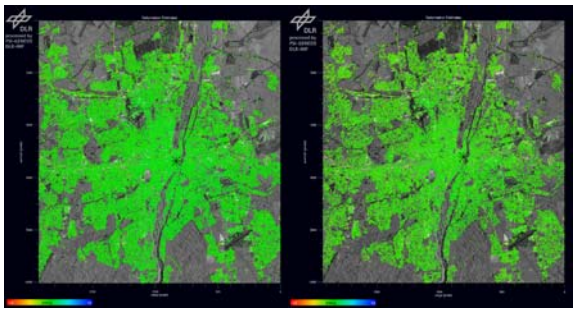

*Figure 10.PSs (left) and CSs (right) velocity displacement map.*

Fig 12 and Fig. 13 show the degree of correlation of the deformation velocity estimation and the topography estimation performed on the pixels common selected by the two techniques. It makes clear that the computation performed on the CSs and on the PSs is very well correlated. Nevertheless, we can note also an offset respect to the 1 to 1 correlation line and a small variance around it. This is due to a different choice of reference points used for the CSs and PSs processing. In particular, to compute the integration of the reference network a reference point it is necessary. All the measures computed on the other PSs or CSs candidates are relative to this pixel that is supposed to be 0 meter high and motionless. However this is only a constant term in the whole estimation that can be eliminated using a Ground Control Point. More important is the noise of this point that is present in each measure, so it is necessary to select it carefully considering its phase dispersion. The noise of the reference point will contribute to the variance around the perfect correlation line because it will propagate trough the network and thus will affect the parameters estimation of the other points. Another contribution to the variance is given by a different extraction of the phase of the pixels (including the reference point) during the processing with the CSs and with PSs point sets In the first case the pixel phase is the one corresponding to the point selected while, in the second case, the PS selection is followed by a point target analysis. Then, the value of the phase corresponds to a sub pixel position.

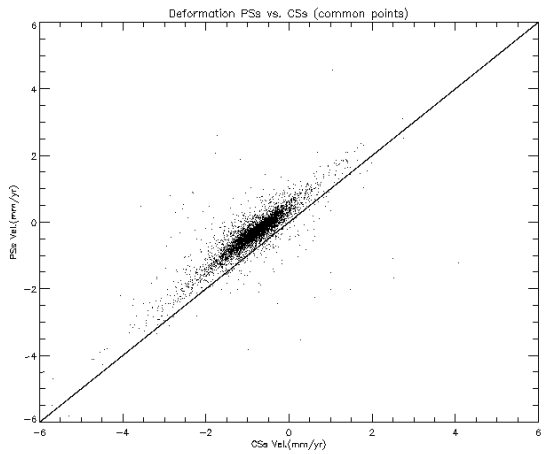


*Figure 12. Correlation of the velocity displacement measured on the common points selected by the two techniques.*

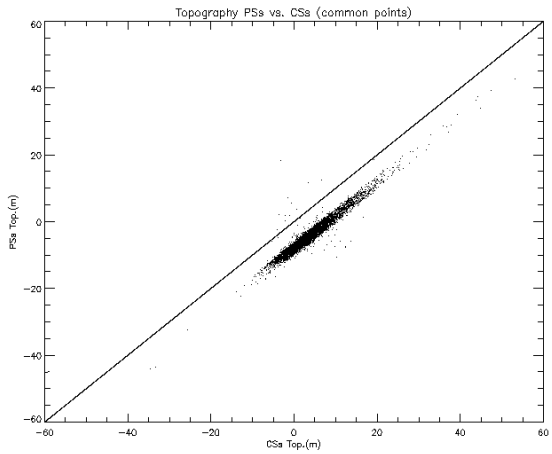


*Figure 13. Correlation of the topography measured on the common points selected by the two techniques.*

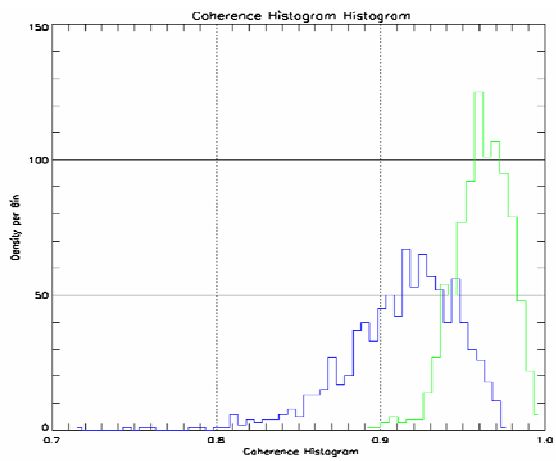


*Figure 14. Final CSs and PSs coherence.*

Another important quality parameter for CSs and PSs is given by their final coherence. This is a measure of how well the finally selected points follow the linear model displacement. Fig. 14 shows the histogram of the final coherence calculated for the CSs (blue line) and the PSs (green line). As we can see the coherence values are over 0.8 for the CSs and 0.9 for the PSs confirming the agreement of the measured displacement with the model for both categories of point-like scatterers.

## 5. CONCLUSIONS

In this paper it has been investigated the temporal behavior of the CSs and their relation with the PSs. A slightly modified CSs detection approach has been used that enabled the detection of many stable CSs. Their time characteristics have been investigated mainly in term of correlation between sub-look coherence and other quantity like signal amplitude and dispersion index. The CSs and PSs location in the scene has been compared. Many points have been found to be located in different positions allowing the possibility to perform a combined detection procedure in order to increase the density of detected points. The LOS velocity displacement and the topography have been evaluated for both the classes of point-like scatterers showing in general a very good agreement. Finally the CSs and PSs coherence values have been computed demonstrating the reliability of the liner displacement model applied to the two categories of points.

## REFERENCES


1. R.Z. Schneider, K.P. Papathanassiou, I. Hajnsek & A. Moreira, “Polarimetric and Interferometric Characterization of Coherent Scatterers in Urban Areas”, *IEEE Trans. Geoscience and Remote Sensing*, vol. 44, No. 4, pp. 971-984, April 2006.

2. A. Ferreti, C. Prati & F. Rocca, “Permanent scatterers in SAR interferometry,” *IEEE Transactions on Geoscience and Remote Sensing*, vol. 39, no. 1, pp. 8-20, January 2001.

3. L. Marotti, R. Z. Schneider, K. P. Papathanassiou, ”Analysis of the Temporal Behaviour of Coherent Scatterers (CSs) in ALOS-PalSAR Data”, IEEE International Geoscience and Remote Sensing Symposium (IGARSS), 23-27 July 2007, Barcelona, Spain.

4. A. Ferreti, C. Prati & F. Rocca, “Nonlinear Subsidence Rate Estimation Using Permanent Scatterers in Differencial SAR Interferometry”,

IEEE Transaction on Geoscience and Remote Sensing, Vol. 38, No. 5, September 2000.

5. N. Adams, B. Kampes, M. Eineder, „Development of a Scientific Permanent Scatterers System: Modifications for ERS/ENVISAT Time Series", in ENVISAT/ERS Symposium (2004).

6. A. Parizzi, "Signal to Clutter Ratio (SCR) Estimation and Side Lobe Suppression for Permanent Scatterers Interferometry", Technical Note.

7. B. M. Kampes, "Displacement Parameter Estimation using Permanent Scatterer Interferometry", PhD Thesis.